

Evaluation of a Conductive Elastomer Seal for Spacecraft

C.C. Daniels¹, J.L. Mather², and H.A. Oravec³

*The University of Akron
Akron, OH 44325-3901, USA*

P.H. Dunlap, Jr.⁴

*NASA Glenn Research Center
Cleveland, OH 44135, USA*

Abstract

An electrically conductive elastomer was evaluated as a material candidate for a spacecraft seal. The elastomer used electrically conductive constituents as a means to reduce the resistance between mating interfaces of a sealed joint to meet spacecraft electrical bonding requirements. The compound's outgassing levels were compared against published NASA requirements. The compound was formed into a hollow O-ring seal and its compression set was measured. The O-ring seal was placed into an interface and the electrical resistance and leak rate were quantified. The amount of force required to fully compress the test article in the sealing interface and the force needed to separate the joint were also measured. The outgassing and resistance measurements were below the maximum allowable levels. The room temperature compression set and leak rates were fairly high when compared against other typical spacecraft seal materials, but were not excessive. The compression and adhesion forces were desirably low. Overall, the performance of the elastomer compound was sufficient to be considered for future spacecraft seal applications.

Nomenclature

a_0	=	zero-order regression coefficient
a_1	=	first-order regression coefficient
β	=	bias error
h_o	=	initial height
h_{70}	=	height after 70 hours
h_{spacer}	=	spacer height
i, k	=	indices
m	=	mass
\dot{m}	=	mass leak rate
N	=	number of samples
p	=	absolute pressure
ϕ	=	precision error
R	=	specific gas constant
T	=	temperature
t	=	time
U	=	uncertainty
V	=	volume

¹ Associate Research Professor, Department of Mechanical Engineering, AIAA Senior Member.

² Senior Research Engineer, College of Engineering.

³ Research Assistant Professor, College of Engineering, AIAA Member.

⁴ Mechanical Engineer, Materials and Structures Division, 21000 Brookpark Rd. MS 23-3.

I. Introduction

AS humans explore deeper into space, the operating environment of gas pressure seals becomes more demanding. The environment is dissimilar from that for terrestrial applications and necessitates development and testing for safe performance. Fortunately, the pressure differential is quite low, typically enclosing atmospheric pressure air within the vehicle with the vacuum of space on the seal's exterior. However, the seal is required to leak as little as possible to conserve limited resources.

In general, gas pressure seals can be manufactured from many materials, but are typically made from various polymers and metals. Two operational characteristics of seals used for spacecraft hatches and docking systems severely limit the materials used in construction. The need to reuse the seal when a hatch repeatedly opens and closes (perhaps hundreds of times) eliminates most seals made from metal. Operational temperature ranges, as broad as -100 to +100°C, greatly reduce the number of usable polymer compounds. As a result of these requirements (and others such as compounds that are low outgassing and those capable of being made into a seal), spacecraft seals are generally manufactured with a silicone compound matrix. Additives are then used to tailor the hardness and improve performance such as durability to ultraviolet radiation and atomic oxygen exposure, low adhesion to the counterface, and abrasion resistance.

Furthermore, NASA-STD-4003A specifies electrical resistivity requirements between two metal interfaces in contact with each other.¹ Electrical conductivity between parts provides a fault current path to protect personnel from electrical shock and protects equipment from lightning strikes. Protection from lightning strikes is addressed under Class L bonding requirements which necessitate the direct current resistance between metal interfaces to be 2.5 milliohms or less. This requirement is applied to all doors, hatches, and access panels comprising the vehicle outer mold line to provide a low impedance enclosure.

The conductivity requirements are typically not a challenge for the gas pressure seals of spacecraft hatches and doors, as doors and hatches are generally thought to close flush to their seat and make metal-to-metal contact completely around their perimeter. However, this may not be the case depending upon the hatch or door design. In an effort to reduce the weight of the hatch (and the spacecraft) the number of latches may be reduced. Combined with the separating force created by the seal, the hatch may deflect, separate from its seat, and lose continuous metal contact resulting in a loss of the continuous electrical pathway. The latches may continue to provide electrical conductivity, but this is not sufficient to meet the requirements of NASA-STD-4003A.

As a result, a gas pressure seal that provides a continuous low-resistance electrical pathway around the entire perimeter of the hatch is desirable. As the seal forms a barrier to gas escaping the vehicle, it makes continuous contact with both the door and its counterface. The selected polymer compound investigated herein was evaluated to determine its potential as an electrically conductive gas pressure seal for spacecraft doors and hatches.

The key characteristics of the elastomer were investigated to evaluate its suitability to form a seal in a non-static spacecraft joint. These characteristics included (1) the amount of outgassed products from the compound when in a heated vacuum-pressure environment, (2) the electrical resistivity of the seal, (3) the compression set of the elastomer compound, (4) the force imposed on the structure by the seal in the formed joint, (5) the adhesion between the seal and its counterface when separated, and (6) the leak rate of the elastomer seal.

II. Test articles

A. General

The elastomer compound was CHO-SEAL® 1285 manufactured by Parker Hannifin Corporation's Chomerics Division (Woburn, MA). The elastomer contains silver-plated aluminum in a silicone matrix. Specimen geometry was a hollow O-ring with nominal cross section dimensions of 6.60 and 11.1 mm inside and outside diameters, respectively. The test articles were cleaned with isopropyl alcohol and allowed to air dry prior to any evaluation.

B. Outgassing

Three samples were fashioned by destructively removing them from a linear segment of the hollow O-ring. The samples had an average mass of 225 mg.

C. Electrical resistivity

One linear segment of the hollow O-ring was used for the measurement of resistivity, similar to Fig. 1(a). The test article was 62.2 cm long and was previously compressed during the compression and adhesion force measurement portions of this study.

D. Compression set

Segments of the hollow O-ring were removed to form 4 cm long test articles for compression set testing, similar to Fig. 1(b). The height of every segment was measured using a non-contact laser profile measurement system, as in Ref. 2, to ensure that the deformable seal was not compressed during the measurement process. The test articles were separated into two lots each with 3 segments. One lot of test articles was lubricated with vacuum grease; the other lot remained unlubricated.

E. Compression force and adhesion force

A linear segment of the hollow O-ring cord was used for the measurement of compression and adhesion forces, similar to Fig. 1(a). The length of the test article was such that it filled the circumferential length of the dovetail groove in which it was tested so that the test article could not deform in the circumferential direction. One test article was used for the compression and adhesion tests.

F. Leak rate

The manufacturer bonded an O-ring cord segment into a toroidal shape to form a continuous seal, similar to Fig. 1(c). This test article was similar to an O-ring seal that would be used for a spacecraft seal application in that it formed a continuous structure. One test article was used for the leak rate tests.

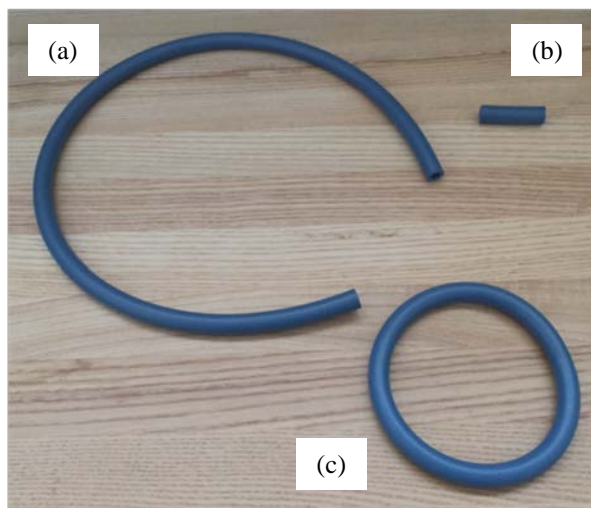


Fig 1. Photograph of test articles similar to those used for testing (a) electrical conductivity, compression force, and adhesion force, (b) compression set, and (c) leak rate.

III. Experimental setup and procedures

A. Outgassing

The outgassing tests were conducted in accordance with ASTM E595-07.³ For the reader's reference, the standard specified that the mass of each sample was recorded before and after exposure to $125 \pm 1^\circ\text{C}$ for 24h in a vacuum of 5×10^{-5} torr or less. The mass of a collector before and after the test was used to calculate the condensed volatiles. A blank control sample was run in parallel to verify no drift occurred in the mass measurement instrument during the duration of the test. The results were quantified in mass percentage.

B. Electrical resistivity

To estimate the electrical resistivity of a structural joint formed using a seal manufactured from the elastomer compound, an elastomer test article was placed between two platens, see Fig. 2. The design of the experimental setup was intended to have only one conductance path between the upper and lower platens, that is, through the elastomer seal. The platens were made of aluminum coated with 0.008 to 0.01 mm thick of class 4, grade A, electroless nickel per SAE-AMS-C-26074,⁴ and were verified to not contribute to the resistance measurement due to their excellent electrical conductance. One electrical lead from a precision milliohm meter was connected to the upper platen, while the other electrical lead was connected to the lower platen. The milliohm meter, Model 380560 manufactured by Extech Technologies, utilized four-wire (Kelvin) electrical clips to eliminate the lead resistance from the measurement. While the measurements were taken, the meter was set to read at its highest resolution and had a full-scale resistance of 20 milliohms. The test article was compressed at three levels by applying additional weight to the upper platen: the upper platen by itself (91 N), the upper platen plus 45 N, and the upper platen plus 89 N.



Figure 2. Photograph of the electrical resistivity measurement setup.

C. Compression set

The compression set of the O-ring segments was measured according to ASTM D395 Method B⁵ guidelines with minimal exceptions. None of the deviations for the standard protocol were expected to significantly alter the results.

The heights of the test articles were measured with a non-contact laser (to 4 decimal places in inch units), similar to Ref. 2, so as to minimize the deformation caused by handling and touching the soft test articles during the measurement process.⁶ Four measurements were made of each test article using a Keyence laser head, model LJ-G200, mounted to a Keyence controller, model LJ-G5001, which displayed the profile reading on an LCD monitor. The average of four height measurements was recorded and the average height of all of the test articles was computed. Spacers, each with a height of three-quarters the average pre-test test article height, were placed between the two platens to control the amount of compression, see Fig. 3.

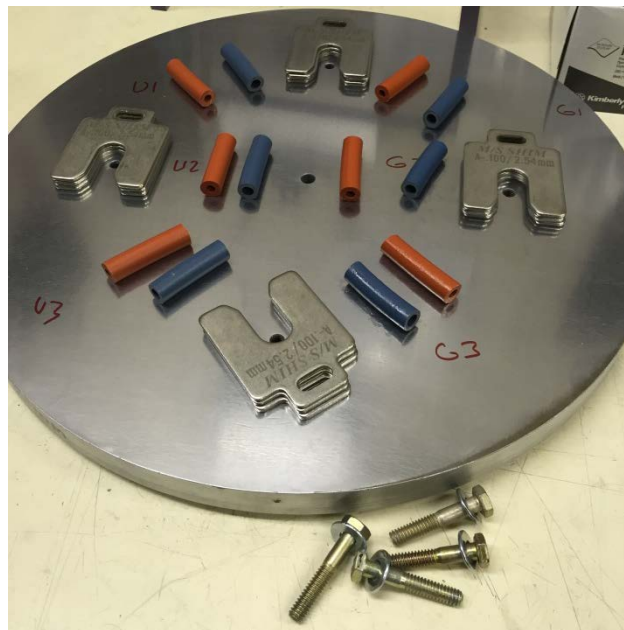


Figure 3. Photograph of the test articles placed on one platen of the compression set measurement setup with spacer shims.

The two steel platens each had a surface finish better than 0.41 μm . The platens, with the specimens squeezed in between, were bolted together and held for 70 hours. Though the temperature and humidity were not continuously monitored, the compressed test article assembly remained in a laboratory environment throughout the test.

After 70 hours, the bolts and upper platen were removed. Contrary to ASTM D395 Method B, the test articles remained on the lower steel platen instead of being placed on a poor thermally conductive surface. Four measurements were made of the test article heights 30 minutes after decompression.

For each test article, the average of four post-test measurements was recorded. The compression set was calculated from Eqn. 1,⁵

$$\frac{h_o - h_{70}}{h_o - h_{spacer}} * 100 \quad (1)$$

In accordance with ASTM D395, the median value from the three test articles was reported as the final compression set measurement.

D. Compression and adhesion forces

The forces needed to compress and separate the seal joint were quantified using an Instron electromechanically actuated load frame controlled by a software program coupled with a 55.6 kN Interface load cell.

The test fixture consisted of two 6061-T6 aluminum plates fixed to the concentrically aligned upper and lower rods of the load frame, Fig. 4. The upper plate was flat, and the lower plate contained a dove-tail groove to receive the O-ring test article. Both plates were clear anodized per MIL-A-8625, Type II, Class 1⁷. Prior to anodization, the surface finish of the plates was better than 16 μin . Prior to testing, each plate was cleaned with an IPA-soaked task wipe.

The test fixtures were contained within an environmental chamber at a nominal temperature of 18.3°C, using liquid nitrogen as the medium for temperature control. The temperature of the test fixture was measured by an Omega resistance temperature device (RTD) with Class A accuracy of $\pm(0.15+0.002t)^\circ\text{C}$, where t is the test temperature in $^\circ\text{C}$.

The forces required to fully compress and separate the seal were measured using a 56 kN load cell mounted above the upper test plate. The load cell was mounted external to the environmental chamber, negating potential error due to elevated or chilled test temperatures. The load cell had a deadband, or uncalibrated range, of $\pm 89\text{ N}$.

The test article was subjected to 10 load cycles where each cycle consisted of three phases: compression, dwell, and separation. Prior to compression, the environmental chamber was purged with dry air and the test assembly was cooled to a nominal temperature of 18.3°C. When the test fixture had reached a steady state temperature, the test article was compressed at a rate of 0.2 mm/s until a nominal applied force of 36 kN was achieved. Compression was held at this constant load until a set dwell time of one minute had expired. The plates were then separated at a rate of 0.25 mm/s. The test article was allowed to recover in an uncompressed state for a duration of one minute and then the subsequent test cycle was started. The test continued in this fashion until all 10 load cycles were completed. After the test was completed, the test article was uninstalled and inspected for any deformations or compression set.

E. Leak rate

The test apparatus consisted of a hermetically sealed volume of gas, except for the test article whose leak rate quantity was of interest. The apparatus was pressurized with dry air at approximately 129 kPa which was allowed to leak past the test article. The low-pressure region was controlled such that a differential pressure across the test article was maintained at 101 kPa throughout the test. This differential pressure was measured using a differential pressure transducer of suitable range, see Fig. 5. As the pressure of the high-pressure region decreased due to leakage past the test article, the pressure in the low-pressure region was reduced by a similar value to maintain the constant differential pressure. A constant differential pressure throughout the duration of the test resulted.

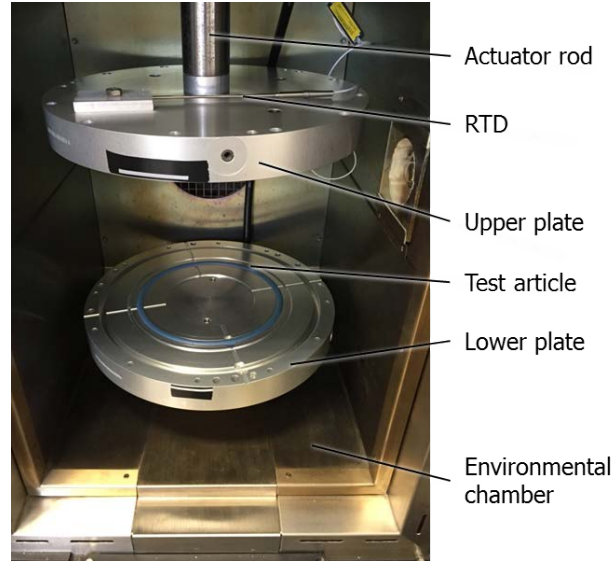


Figure 4. Photograph of the compression and adhesion force measurement test fixture.

A controller managed the activity of the pressure regulator. The input value from the differential pressure transducer was compared to the desired set point. Using a proportional-integral control algorithm, the controller sent a voltage signal to the pressure regulator, with connections to both an ambient pressure vent and vacuum, to raise or lower the downstream pressure as appropriate to obtain the desired pressure differential, 101 kPa, across the test article.

To minimize any errors between the temperature measurements and the actual gas temperature, the test section, pressure transducers, volume, RTD, and hermetic valve were contained within an environmental control chamber. The environmental control chamber then was set to the desired test temperature and kept the temperature of the apparatus constant throughout the duration of the experiment.

The gas pressure and temperature within the high-pressure side volume were recorded over time. The mass point leak rate method was used to analyze the data and obtain the leak rate result and its uncertainty.⁸ Using *Boyle's law*, the volume was quantified in advance.⁹ The *ideal gas law* was assumed, and the mass of gas within the system was calculated using Eqn. 2 for each time-step yielding a mass-time data set.

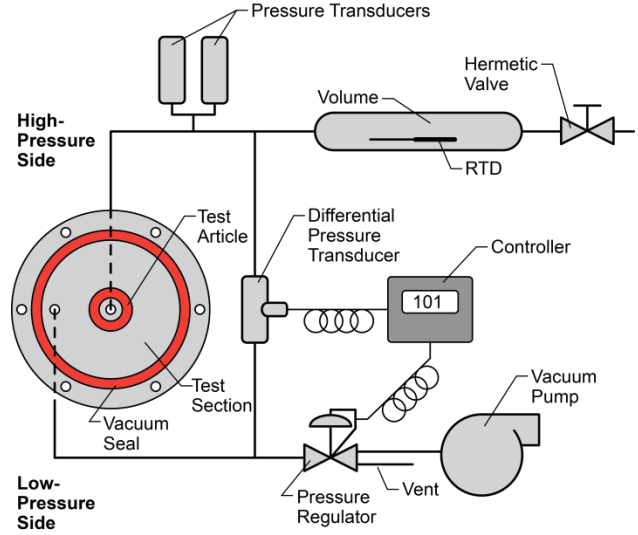


Figure 5. Diagram of the leak rate measurement test apparatus.

$$m = \frac{pV}{RT} \quad (2)$$

Since the differential pressure across the test article was the desired value throughout the duration of the test, a linear least-squares regression was computed for the entire data set using Eqn. 3.

$$m(t) = a_1 t + a_0 \quad (3)$$

The uncertainty of mass loss was calculated using Eqns. 4 and 5.¹⁰

$$U_m^2 = \sum_{i=1}^N \left(\frac{\partial \dot{m}}{\partial m_i} \right)^2 \beta_{m_i}^2 + \sum_{i=1}^N \left(\frac{\partial \dot{m}}{\partial m_i} \right)^2 \phi_{m_i}^2 \quad (4)$$

where,

$$\begin{aligned} \beta_m^2 &= \left(\frac{V}{RT} \beta_p \right)^2 + \left(\frac{p}{RT} \beta_V \right)^2 + \left(\frac{pV}{R^2 T} \beta_R \right)^2 + \left(\frac{pV}{RT^2} \beta_T \right)^2 \\ \phi_m^2 &= \left(\frac{V}{RT} \phi_p \right)^2 + \left(\frac{p}{RT} \phi_V \right)^2 + \left(\frac{pV}{R^2 T} \phi_R \right)^2 + \left(\frac{pV}{RT^2} \phi_T \right)^2 \end{aligned} \quad (5)$$

and

$$\frac{\partial \dot{m}}{\partial m_i} = \frac{N t_i - \sum_{i=1}^N t_i}{N \sum_{i=1}^N (t_i^2) - (\sum_{i=1}^N (t_i))^2}$$

Using this method, the leak rate and associated uncertainty (using Eqns. 2-5) was computed at each time step in real-time.

IV. Results and Discussion

A. Outgassing results

The values for total mass loss (TML) and collected volatile condensable materials (CVCM) are shown in Table 1. The compound met the outgassing requirements for spacecraft materials as defined in Ref. 3, having a TML of less than 1.0% and a CVCM value less than 0.1% after 24 hours.

Table 1. Measurements of outgassing characteristics.

TML, %	CVCM, %
0.041	0.014

B. Electrical resistance results

The electrical resistance of the assembly, as shown in Table 2, was 0.62 milliohms with 89 N of additional weight added to the upper platen. This was negligibly less than the 0.70 milliohms value measured with only the force of the upper plate compressing the test article and indicated that compressing the seal had little effect on the resistance of the assembled joint. All of the tested assemblies met the requirements of less than 2.5 milliohms as dictated by Ref. 1. It should be noted that resistance is dependent on material resistivity, length, and cross section. So while the measured resistance values were less than 2.5 milliohms, the resistance was specific to the test setup utilized herein and may vary if the seal is used in other hardware configurations. These results suggested that the elastomer is capable of conducting electrical charge with minimal resistance if there were no other structural pathways on the spacecraft.

Table 2. Electrical resistance measurements of linear segments.

Configuration (total force)	Resistance, milliohms
Upper platen only (91 N)	0.70
Platen plus 45 N (136 N)	0.66
Platen plus 89 N (180 N)	0.62

C. Compression set results

The compression set measurements of the seal segments were relatively high, as shown in Table 3, as compared to other silicone elastomers which are typically in a range from 5 to 11%.¹¹ The lubricated test articles exhibited less compression set than those that were unlubricated. This was expected as the lubrication reduced the amount of stress within the test article and allowed for greater deformation when compared to a non-lubricated test article placed under similar loading (not displacement) boundary conditions. It is time under a stress field that causes the molecular chains of the test article to reorient which is observed as compression set.

Table 3. Compression set results of linear segments following ASTM D395 Method B procedures.

	Unlubricated	Lubricated
Compression set measurement	15.3%	14.0%

The test articles included in this study were batched with others from another study such that the spacer height (8.03 mm) was 0.743 times the average pre-test height (11.2 mm). This value was negligibly different than the target value of 0.750 times the average.

Before this elastomer can be utilized as a compound for seals used in space applications, the compression set must be further evaluated since the standard test method does not adequately represent any application. Firstly, due to the higher than typical compression set shown above, the compression set at the limits of the temperature operating range must be determined, similar to other studies.¹¹⁻¹² The immersion in different thermal environments may cause higher compression set levels that must be accounted for in joint design. Secondly, compression set for durations longer than those utilized herein should also be investigated, as longer durations may cause higher compression set.¹²

D. Compression force results

The amount of force required to compress the seal was measured at 18.3°C. The test measured the force during both the compression and decompression motions of the load frame, such that compression and adhesion force measurements were generated during each cycle. Ten total cycles were conducted, and the compression force values for each are tabulated in Table 4 and graphically depicted in Fig. 6.

The soft elastomer compound and the hollow O-ring design resulted in very low force needed to compress the seal, less than 17.6 N/cm (including maximum uncertainty). This low force could be very desirable for spacecraft

applications and was lower than that measured for other designs and compounds.¹³ Additionally, the compression force was consistent throughout the ten cycles investigated, another desirable characteristic.

It is critical to compare the reported force values against the calibrated range of the load cell measurement device to ensure that the experimental setup and instruments were appropriate. Repeated experiments after experimental modifications are common, especially when both tension and compression measurements are made within the same experiments. The challenge to properly configure the design becomes greater when the tension and compression forces have a large difference in magnitude, as it was in these experiments. Combining the deadband of the load cell, ± 89 N, with the weight of the actuator rod and upper plate resulted in an uncalibrated range of +89 to +270 N. Since the total compression force measurements (incorporating the weight of the rod and plate) were outside the deadband range, +658 to +761 N, the reported values were verified to be accurate.

An investigation of the force response over time was outside the scope of this work. In order to design the seal joint, a better understanding of the stability of the compression force with time will be necessary as residual seal load is known to decrease with time.¹⁴ Since the force value is so low, any reduction in this value may cause the leak rate to rise at the interface between the elastomer and the seal groove or between the elastomer and counterface.

Table 4. Measurements of force needed to compress the seal against its counterface.

Cycle number	Compression force, N/cm	Uncertainty, N/cm
1	15.1	± 2.5
2	14.5	± 2.5
3	14.2	± 2.5
4	14.0	± 2.5
5	13.5	± 2.5
6	13.8	± 2.5
7	13.5	± 2.5
8	13.7	± 2.5
9	13.7	± 2.5
10	13.7	± 2.5

Table 5. Measurements of adhesion force upon separating the seal from its counterface.

Cycle number	Adhesion force, N/cm	Uncertainty, N/cm
1	-0.08	+0.08 / -0.6
2	-0.07	+0.08 / -0.6
3	-0.08	+0.08 / -0.6
4	-0.07	+0.08 / -0.6
5	-0.07	+0.08 / -0.6
6	-0.08	+0.08 / -0.6
7	-0.07	+0.08 / -0.6
8	-0.07	+0.08 / -0.6
9	-0.08	+0.08 / -0.6
10	-0.07	+0.08 / -0.6

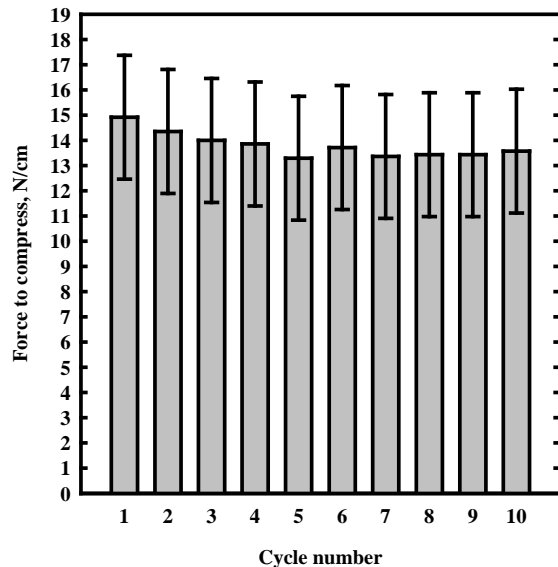


Figure 6. Force required to compress the seal. Error bars represent measurement uncertainty.

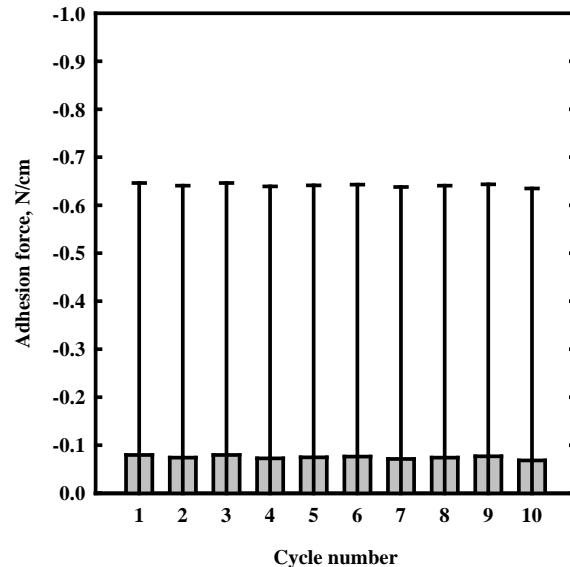


Figure 7. Adhesion between seal and anodized aluminum counter-face. Error bars represent measurement uncertainty.

E. Adhesion force results

During the decompression stroke of the load frame, the load cell was used to quantify any adhesion between the elastomer seal and its anodized aluminum counterface surface. The values are tabularized in Table 5 and shown graphically in Fig. 7. The force generated by adhesion was very low and not significantly different than zero. This characteristic was very desirable as it minimizes or eliminates the need for a mechanism to separate the joint, if needed, during the spacecraft's mission.

The adhesion forces observed were checked against the calibrated range of the load cell, similar to the procedures used previously. The total adhesion force measured by the load cell, approximately -188 N, was outside the uncalibrated deadband range of the load cell, +89 to +270 N. Therefore, the reported adhesion values were accurate.

F. Leak rate results

The leak rate of the O-ring was quantified at two temperatures, 23 and 61°C, as the permeation rate of elastomers is highly dependent upon test temperature.¹⁵ The leak rate results are quantified in Table 6 and shown graphically in Fig. 8. As expected, the leak rate was elevated at the warmer test temperature.

The overall magnitude of the leak rates was relatively high compared with the requirement historically used by NASA. This was somewhat expected from the hollow O-ring design since the gas volume in the centrally located void provides no resistance to permeation flow. Additionally, the force required to compress the seal, shown previously, was low which allowed for increased leakage through the interface between the seal and counterface.

The measurement uncertainty of the leak rate measurements were very low, 1.58% and 0.918%, for the room and elevated temperature cases, respectively.

V. Summary and Future Work

An electrically conductive elastomer was investigated to evaluate its material properties and performance characteristics for applications as a space seal. The amount of outgassing from the elastomer was determined. The level of compression set and the electrical conductance of test articles formed into a hollow O-ring shape were measured. The level of adhesion between a seal and its counterface, the amount of force to fully compress a seal, and the leak rate of a seal were quantified.

The results of the outgas testing indicated that little of the compound was volatilized during exposure to heat and vacuum, easily meeting the 1.0% TML and 0.1% CVCM specifications of ASTM E595-07. The electrical resistance of the elastomer compound was measured to be less than 1 milliohm and was therefore deemed excellent. The very low resistive path between two metal plates met the Class L bonding requirement of less than 2.5 milliohms. The hollow O-ring seal manufactured from the compound required a low amount of force to compress in the sealed joint, approximately 15 N/cm. The seal adhered to the counterface a negligible amount when separated. The air leak rates at room and elevated temperatures were 258 and 358 ng/s, respectively, and would be expected to meet most spacecraft requirements when fully compressed.

Depending upon the specific spacecraft application, several characteristics of the elastomer must be evaluated. As described previously, longer duration compression force and set measurements should be made to properly design the seal joint. Additionally, if the seal application includes exposure to space environments (e.g., atomic

Table 6. Leak rate measurements.

Temperature °C	Leak rate ng/s	Uncertainty ng/s
+23	258	4.08
+61	358	3.28

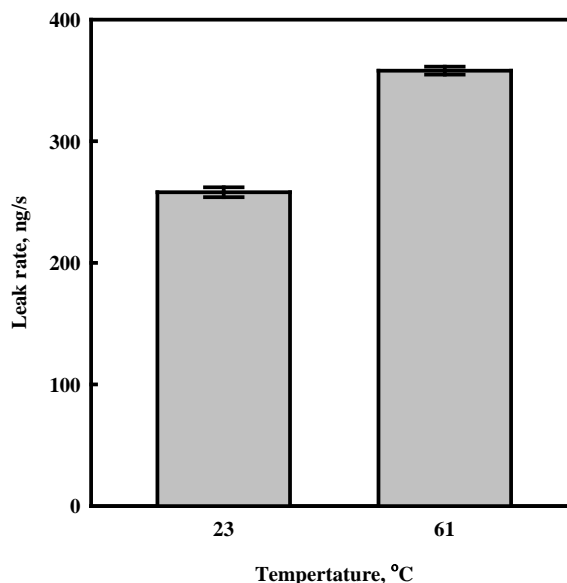


Fig. 8 Leak rate results of O-ring seals at two temperatures. Error bars represent measurement uncertainty.

oxygen, ultraviolet radiation, and/or ionizing radiation), the degradation due to these exposures must be ascertained as these environments have been shown to affect seal performance.^{11,16} The adhesion between the elastomer and the counterface must be investigated after durations greater than one minute, since the joint will likely be closed for much longer time periods and adhesion increases with time.¹⁷ If the sealed joint is to be mated during the mission and the elastomer is unprotected from micrometeoroids and orbital debris, the effects of impacts should also be characterized.¹⁸ Lastly, the silver-plated aluminum filler material that provided the electrical conductivity to the seal must be rated as acceptable for use in spacecraft hardware.

VI. Acknowledgements

The authors wish to thank Nathan S. Williams for his assistance with the electrical resistance measurements. We also thank John J. Mayer and Joseph P. Assion of Vantage Partners, LLC for their engineering design support. Funding for this work was provided by the National Aeronautics and Space Administration under contract NNC13BA10B.

VII. References

- ¹NASA-STD-4003A, "Electrical Bonding for NASA Launch Vehicles, Spacecraft, Payloads, and Flight Equipment." National Aeronautics and Space Administration, Washington, DC, 2013.
- ²Taylor, S.C., "Noncontacting Laser Inspection System for Dimensional Profiling of Space Application Thermal Barriers," NASA/CR-2011-216803, Washington, D.C., 2011.
- ³ASTM Standard E595, 2003e2, "Standard Test Method for Total Mass Loss and Collected Volatile Condensable Materials from Outgassing in a Vacuum Environment," ASTM International, West Conshohocken, PA, 2003.
- ⁴SAE Standard SAE-AMS-C-26074, "Electroless Nickel Coatings," SAE International, Warrendale, PA, 2013.
- ⁵ASTM D395-14, "Standard Test Methods for Rubber Property—Compression Set," ASTM International, West Conshohocken, PA, 2014.
- ⁶Bastrzyk, M.B., Wasowski, J.L., and Daniels, C.C., "Non-contact Compression Set Testing and Dimensional Measurements of Space Seals: An Application of Laser Technology," *4th Japan-US Symposium on Emerging NDE Capabilities for a Safer World*, M2-1, Columbus, OH, 2010.
- ⁷Military Standard MIL-A-8625F, "Anodic Coatings for Aluminum and Aluminum Alloys," 10 Sep 1993.
- ⁸Garafolo, N. G., "A Compressible Advection Approach in Permeation of Elastomer Space Seals," Ph.D. Dissertation, Univ. of Akron, Akron, OH, 2010.
- ⁹Daniels, C., Braun, M., Oravec, H., Mather, J., and Taylor, S., "Leak Rate Quantification Method for Gas Pressure Seals with Controlled Pressure Differential," *51st AIAA/ASME/SAE/ASEE Joint Propulsion Conference*, AIAA-2015-4231, AIAA, Washington, DC, 2015.
- ¹⁰Garafolo, N.G., and Daniels, C.C., "Mass Point Leak Rate Technique with Uncertainty Analysis," *Research in Nondestructive Evaluation*. 25 (2) 2014: 125–149.
- ¹¹Daniels, C., de Groh III, H., Dunlap, P., Finkbeiner, J., Steinetz, B., Bastrzyk, M., Oswald, J., Banks, B., Dever, J., Miller, S., and Waters, D., "Characteristics of Elastomer Seals Exposed to Space Environments," *43rd AIAA/ASME/SAE/ASEE Joint Propulsion Conference and Exhibit*, AIAA 2007-5741, AIAA, Washington, DC, 2007.
- ¹²Bastrzyk, M., Daniels, C. Oswald, J., Dunlap, P. and Steinetz, B., "Material Properties of Three Candidate Elastomers for Space Seals Applications," NASA/TM-2010-216263, 2010.
- ¹³Bastrzyk, M.B., Garafolo, N.G., and Daniels, C.C., "Compression Force Response and Leak Rate Quantification of Candidate Static Silicone Space Seals," *46th AIAA/ASME/SAE/ASEE Joint Propulsion Conference and Exhibit*, AIAA-2010-6908, Washington, DC, 2010.
- ¹⁴Clinton, R.G., and Turner, J.E., "Long-Term Compression Effects on Elastomeric O-ring Behavior," *AIAA/ASME/ASCE/AHS/ASC Structures, Structural Dynamics and Materials Conference*, AIAA-90-1110-CP, AIAA, Washington, DC, 1990.
- ¹⁵Garafolo, N., and Daniels, C., "An Experimental Investigation of Leak Rate Performance of a Subscale Candidate Elastomer Docking Seal," *46th AIAA/ASME/SAE/ASEE Joint Propulsion Conference and Exhibit*, AIAA 2010-6907, AIAA, Washington, DC, 2010.
- ¹⁶Christensen, J.R., Underwood, S.D., Kamenetzky, R.R., and Vaughn, J.A., "Atomic Oxygen Effects on Seal Leakage," *20th Space Simulation Conference: The Changing Testing Paradigm*, 27–29 Oct 1998, Annapolis, MD.

¹⁷Hartzler, B., Panickar, M., Wasowski, J. and Daniels, C., "Comparison of Adhesion and Retention Forces for Two Candidate Docking Seal Elastomers," *52nd AIAA/ASME/ASCE/AHS/ASC Structures, Structural Dynamics and Materials Conference*, AIAA 2011-2158, AIAA, Washington, DC, 2011.

¹⁸de Groh III, H.C., and Steinetz, B.M., "Effects of Hypervelocity Impacts on Silicone Elastomer Seals and Mating Aluminum Surfaces," *45th AIAA, ASME, and ASEE Joint Propulsion Conference and Exhibit*, AIAA-2009-5249, AIAA, Washington, DC, 2009.